Generation of high pressure shocks relevant to the shock-ignition intensity regime

D. Batani, L. Antonelli, S. Atzeni, J. Badziak, F. Baffigi, T. Chodukowski, F. Consoli, G. Cristoforetti, R. De Angelis, R. Dudzak, G. Folpini, L. Giuffrida, L. A. Gizzi, Z. Kalinowska, P. Koester, E. Krousky, M. Krus, L. Labate, T. Levato, Y. Maheut, G. Malka, D. Margarone, A. Marocchino, J. Nejdl, Ph. Nicolai, T. O'Dell, T. Pisarczyk, O. Renner, Y. J. Rhee, X. Ribeyre, M. Richetta, M. Rosinski, M. Sawicka, A. Schiavi, J. Skala, M. Smid, Ch. Spindloe, J. Ullschmied, A. Velyhan, and T. Vinci

Citation: Physics of Plasmas (1994-present) **21**, 032710 (2014); doi: 10.1063/1.4869715
View online: http://dx.doi.org/10.1063/1.4869715
View Table of Contents: http://scitation.aip.org/content/aip/journal/pop/21/3?ver=pdfcov
Published by the AIP Publishing

Generation of high pressure shocks relevant to the shock-ignition intensity regime

D. Batani,[1] L. Antonelli,[1,2] S. Atzeni,[3] J. Badziak,[4] F. Baffigi,[5] T. Chodukowski,[4] F. Consoli,[6] G. Cristoforetti,[5] R. De Angelis,[6] R. Dudzak,[7] G. Folpini,[1] L. Giuffrida,[1] L. A. Gizzi,[5] Z. Kalinowska,[4] P. Koester,[5] E. Krousky,[7] M. Krus,[8,9] L. Labate,[5] T. Levato,[2,8] Y. Maheut,[1] G. Malka,[1] D. Margarone,[8] A. Marocchino,[3] J. Nejdl,[8] Ph. Nicolai,[1] T. O'Dell,[10] T. Pisarczyk,[4] O. Renner,[8] Y. J. Rhee,[11] X. Ribeyre,[1] M. Richetta,[2] M. Rosinski,[4] M. Sawicka,[8] A. Schiavi,[3] J. Skala,[7] M. Smid,[8,9] Ch. Spindloe,[10] J. Ullschmied,[7] A. Velyhan,[8] and T. Vinci[12]
[1]*Université Bordeaux, CNRS, CEA, CELIA (Centre Lasers Intenses et Applications), UMR 5107, F-33405 Talence, France*
[2]*Università di Roma "Tor Vergata," Roma, Italy*
[3]*Dipartimento SBAI, Université di Roma "La Sapienza" and CNISM, Roma, Italy*
[4]*Institute of Plasma Physics and Laser Microfusion, Warsaw, Poland*
[5]*Intense Laser Irradiation Laboratory, INO-CNR, Pisa, Italy*
[6]*CRE, ENEA, Frascati, Italy*
[7]*Institute of Plasma Physics of the ASCR, PALS, Za Slovankou 3, 182 00 Prague, Czech Republic*
[8]*Institute of Physics of the ASCR, ELI-Beamlines/HiLASE/PALS, Na Slovance 2, 182 21 Prague, Czech Republic*
[9]*Czech Technical University, Prague, Czech Republic*
[10]*Scitech Precision Ltd, Rutherford Appleton Laboratory, Harwell Oxford, Didcot, Oxon, OX11 0QX, United Kingdom*
[11]*Korea Atomic Energy Research Institute, Daejeon 305-353, South Korea*
[12]*LULI, Ecole Polytechnique CNRS, Palaiseau, France*

(Received 12 October 2013; accepted 10 March 2014; published online 31 March 2014)

An experiment was performed using the PALS laser to study laser-target coupling and laser-plasma interaction in an intensity regime $\leq 10^{16}$ W/cm^2, relevant for the "shock ignition" approach to Inertial Confinement Fusion. A first beam at low intensity was used to create an extended preformed plasma, and a second one to create a strong shock. Pressures up to 90 Megabars were inferred. Our results show the importance of the details of energy transport in the overdense region.
 [http://dx.doi.org/10.1063/1.4869715]

I. INTRODUCTION

Shock ignition (SI)[1–5] is a novel approach to Inertial Confinement Fusion (ICF),[6–8] based on the separation of compression and ignition phases. The first phase requires compression of a DT pellet by ns laser beams at $I < 10^{15}$ W/cm^2. The second relies on a laser pulse at $I \approx 10^{15}$–10^{16} W/cm^2, driving a very strong shock (P ≈ several 100 Megabars) generating the hot spot required for ignition. SI has potential for high gain and could also enable ignition at moderate laser energy compared to those expected for currently explored schemes.

Several experiments have shown that compression to a regime of interest for ICF is possible.[9–12] Achieving ignition by creating a central hot spot at the end of the implosion is the objective of the National Ignition Campaign[12] at the National Ignition Facility, NIF, (Ref. 13). It requires, *inter-alia*, the achievement of a high implosion velocity, about 370 km/s for the NIF baseline target. Separation of compression and ignition would allow a lower implosion velocity,[1] reducing risks associated to hydrodynamic instabilities. Such a separation is also common to fast ignition.[14,15] However, SI has the unique advantage that a full scale proof of the scheme is compatible with present-day "NIF like" laser technology.[2,13,16] Also, it does not rely on non-scalable physics as fast ignition (i.e., generation of an intense electron beam, its propagation in dense matter, and energy deposition in the compressed core). Preliminary SI experiments in spherical geometry[17–19] are encouraging and demonstration experiments are possible within the next decade on NIF or Laser Megajoule (LMJ).[20]

However, the physics related to SI was only marginally explored in the past decades. Laser-plasma interactions at intensities $>10^{14}$ W/cm^2 are strongly non-linear. Strong parametric instabilities (Stimulated Brillouin Scattering, SBS, Stimulated Raman Scattering, SRS, and Two-Plasmon Decay, TPD) may arise,[21–23] with the unwanted effect of reflecting a large part of incident laser light and generating fast electrons. These electrons may preheat the target, making compression more difficult. Also, laser filamentation may produce strong inhomogeneities, altering compression uniformity, and enhancing parametric instabilities growth.[24]

We observe that in the new context of SI, the generation of moderately energetic fast electrons may be tolerated or even beneficial to shock generation.[1,25] Indeed, they are produced when most of compression has already occurred and may not be able to penetrate the large areal density $\langle \rho r \rangle$ achieved at this time.

While, of course, SI demonstration experiments need spherical geometry, many underlying issues can be addressed with planar targets. 1D planar geometry offers the advantage of a simpler scheme and easier access of diagnostics. In this context, some results have been reported in Ref. 26, for intensities $\leq 10^{15}$ W/cm^2.

In this article, we report experimental results in the intensity range from 10^{15} to 3×10^{16} W/cm^2 obtained using two beams of the Prague Asterix Laser System, PALS.[27] The goals were to study: (a) the coupling of the high-intensity beam to the payload through an extended plasma and the generation of a strong shock; (b) the effect of laser-plasma instabilities at I$\approx10^{16}$ W/cm^2 and the amount of reflected light; and (c) the generation of hot electrons and their impact on laser-payload coupling.

Here, we mainly focus on point (a), while the full details will be described elsewhere. The experiment was divided in two phases, the first dedicated to the creation of the extended plasma and its characterization and the second to measure shock formation and laser-plasma interaction. Some preliminary results were already presented in Refs. 28 and 29.

II. EXPERIMENTAL SET-UP

The overall scheme of the experimental set-up, as well the scheme of the targets used in the experiment is shown in Fig. 1. The PALS Iodine Laser delivers pulses with wavelength $\lambda=1.3\,\mu$m and $\tau=300$ ps.[25] In the experiment, we used an *auxiliary* beam delivering ≈30 J, and the *main* beam delivering up to 250 J, with delay up to 1.2 ns with respect to the auxiliary beam (see below). The auxiliary beam was operating at the fundamental frequency and focused to I$\approx10^{13}$ W/cm^2 in an extended spot (≈900 μm) to create an approximately 1D plasma. The beam was smoothed with a random phase plate (RPP) to produce a uniform irradiation.

The main beam was used in Phase 1 to create an X-ray laser (XRL) beam for diagnostics.[30] In Phase 2, it was converted to 3ω (E$\leq$250 J and $\lambda=438$ nm) and focused with an F/2 lens of diameter 30 cm and focal length $f=60$ cm to create a strong shock. A phase plate produced a Gaussian spot with 100 μm FWHM at intensity up to 9×10^{15} W/cm^2. For shots at higher intensities, the plate was removed giving a spot with an average diameter of 60 μm and an intensity up to 3×10^{16} W/cm^2. However, without the phase plate the intensity distribution in the focal spot showed the presence of hot spots.

In the experiments, we used different kinds of targets. In particular, we used two-layer targets with 25-μm plastic (parylene-C; C_8H_7Cl, with Cl to allow for X-ray spectroscopy) on the laser side, and 25 μm Al on the rear, and targets with an intermediate Cu layer (5 μm thick) between plastics and Al allowing for hot electron detection. We also used targets with an additional 10 μm Al step on the back allowing for shock chronometry (Al being a standard material for this kind of measurements[31]). The low-Z material on the front mimicked the typical ICF ablator material. Also, we used targets with different plastic thickness in front of the Cu layer: these allowed the average energy of hot electrons to be estimated by looking at the signal reduction vs. overcoat thickness.

Shock chronometry, based upon measurement of self-emission from target rear side using a streak camera,[32] was the primary shock diagnostic. Other diagnostics included ion collectors, optical spectroscopy and calorimetry, and Kα imaging.[33] Optical interferometry was used to monitor the underdense plasma *on-line*.[34] X-ray pin-hole cameras (PHC) provided the transverse size of preformed plasma. High-resolution X-ray spectroscopy, spatially resolved in direction perpendicular to the target, provided the plasma temperature.[35]

III. EXPERIMENTAL RESULTS, CHARACTERIZATION OF THE PREFORMED PLASMA

2D plasma density profiles (see Fig. 2) were obtained with XRL deflectometry,[27,36] a technique based on the deformation of Talbot patterns of a 2D grating caused by gradients of index of refraction (plasma electron density). The details are described in Ref. 28 and some results in Ref. 29. A Ne-like zinc XRL was used, emitting 21.2 nm, 150-ps, and 200 μJ pulses. A Mo-Si multilayered spherical mirror with $f=250$ mm imaged the plasma on a back-illuminated X-ray CCD with magnification M = 8.2.

The plasma with $n_e>10^{20}$ cm^{-3} extends over 200 μm perpendicularly to target surface and over 800 μm radially (comparable to the spot size), in agreement with X-ray PHC images. Such profiles are satisfactorily reproduced by 2D hydro simulations performed with the codes MULTI2D,[37,38] DUED,[39,40] and CHIC.[41]

As for temperature, X-ray keV spectra analyzed with the help of the codes FLYCHK[42] and SPECT3D,[43] yielded ≈700 eV, with the main beam, and ≈200 eV, with the creation beam alone, in the overdense region ($n_e\approx2\times10^{22}$ cm^{-3}), in fair agreement with simulations predictions.

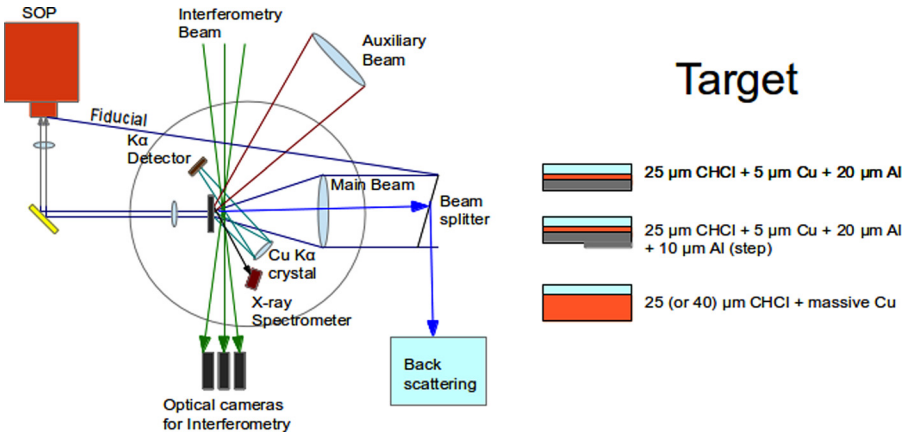

FIG. 1. (on the left) Scheme of the experimental set-up and of the diagnostics; (on the right) the main type of targets used in the experiment.

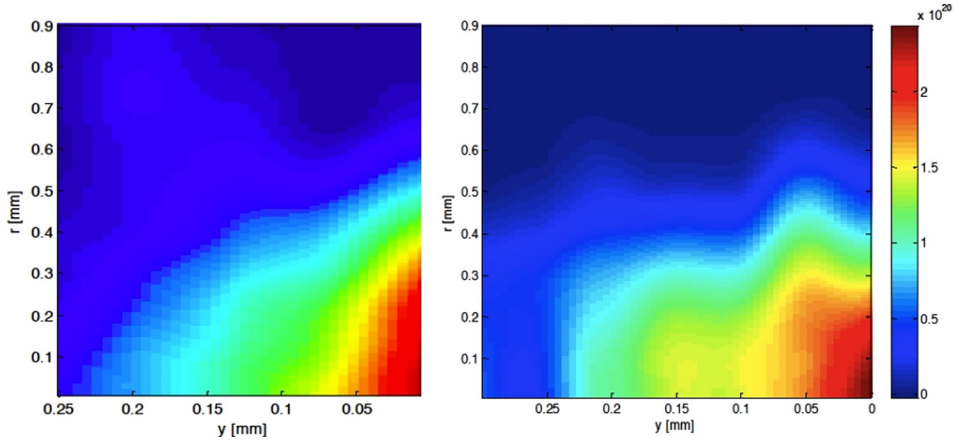

FIG. 2. Experimental results from XRL deflectometry: 2D density electron density profiles (in cm^{-3}) at 0.3 ns (left) and 0.9 ns (right) after the arrival driving pulse.

The ion collectors[44,45] were used to estimate the temperature of the plasma corona with the main beam on, providing values (≈1–2 keV).

The main pulse was fired in the preformed plasma with delays $\Delta t = 0$, 150, 300, 500, 600, and 1200 ps. We also fired shots without the creation beam (main only).

IV. EXPERIMENTAL RESULTS, MAIN BEAM INTERACTION

Fig. 3 shows a streak camera image of a shock breakout obtained from a stepped target. Here, the vertical axis is time (time flows from top to bottom) and the horizontal axis is space. The signal on the top right is a time fiducial, which is obtained by sending a small fraction of the incoming laser beam to the streak camera slit with an optical fiber. Its position represents the time of arrival of the laser beam on the target front side. The two other signals represent the shock breakout from the base and the shock breakout from the step, respectively, as described in Ref. 32. Therefore, on the same laser shots, we get two measurements: the time needed by the shock to cross the base thickness and the time needed to cross the whole target thickness. These two times must be compared to hydrodynamic simulations in order to retrieve the initial value of shock pressure. The step configuration also allows the average shock velocity in the step to be measured directly (given by the step thickness divided by the time difference between shock breakout on the base and on the step). Now, it is well known that the from shock velocity we can retrieve the value of shock pressure if an equation of state (EOS) model is used for the step material (in our case, we used the SESAME tables[46]). However, in our case the measured value of velocity is only an average value (the shock is non stationary) and so is the value of shock pressure inferred in this way. For instance, the velocity from Fig. 3 is ≈20 μm/ns, corresponding to a pressure ≈6 Megabars. Such value, measured at the target rear, is much lower than the shock pressure produced on target front side during laser interaction. Indeed, in our experiment, pressure is rapidly decreasing as the shock propagates in the target. This is partly due to 2D effects as the target thickness is comparable to the focal spot radius (shock propagation changes from planar to spherical). But above all, pressure is not maintained due to the short duration of the laser pulse (a relaxation wave is generated on the front side at the end of the pulse and rapidly catches up with the shock front). Because of the laser interaction condition, high intensity, small focal spot, and the physical conditions are not easy to model. Due to strong 2D effects and the laser pulse shape the pressure decreases rapidly from 350 ps and the drops to 70% to after 500 ps of propagation.

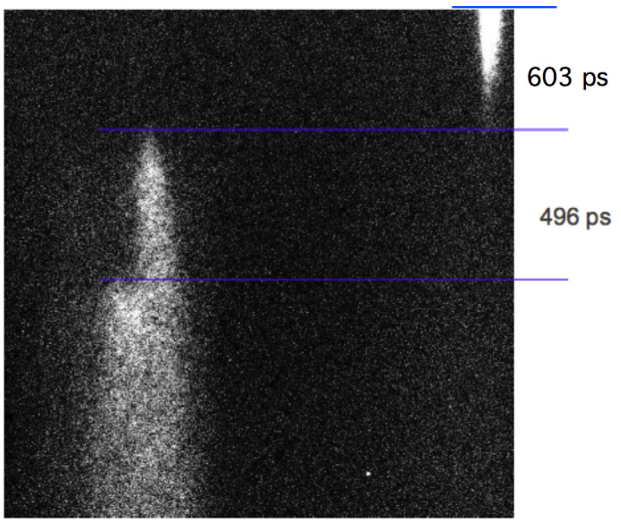

FIG. 3. Shock breakout image for a stepped target with $E(3\omega) = 245$ J, E pre-pulse = 29 J, and delay between auxiliary and main beam 500 ps (shot without phase plate on main beam).

Thinner targets could marginally help in this respect (apart from target fabrication constraints). On the other side, thinner targets would be more sensitive to the problem of preheating. As discussed in details below, hot electrons with energies of about 50 keV are generated in our experimental conditions, which have a range of about 30 μm in plastic. Therefore, too-thin targets would be preheated, and this would mean that one would not be able to use the Hugoniot relations to infer the shock pressure once the shock velocity is measured.

Finally, in order to recover the initial value of shock pressure, starting from experimental data of shock breakout time vs. target and laser parameters, we performed 2D hydro simulations and varied the initial pressure so to reproduce the breakout time. Simulations indicate that the maximum pressure generated in the plastic layer is ≈90 Megabars, and due to the impedance mismatch, it increased up to ≈130 Megabars for the case of Al and ≈210 Megabars for the case of Cu.

Since our estimation of initial shock pressure relies on hydro simulations, it is very important to check that this value does not depend on simulations details. Here, uncertainties come from the flux limiter value, the material EOS, and laser absorption. However, the codes used in hydrodynamic simulations of our experiments have all been benchmarked against several experimental results. Even more importantly, 3 different codes (MULTI2D, CHIC, and DUED) practically give the same results, making us confident in our results.

Copper Kα emission was measured with a spherically bent quartz (211) used in the second crystallographic order, set up as a monochromator in imaging mode (Bragg angle $\theta = 88.7°$) to provide the distribution of Kα intensity, 2D-spatially resolved on target surface. Both such diagnostics and the X-ray spectrometer used Kodak AA400 film. Results from X-ray PHC and Kα imager allowed us to confirm the focusing of the main beam to the expected spot diameter. By using a pin-hole camera CCD in single photon detection mode,[47,48] we obtained low resolution, large spectral range X-ray spectra, and monochromatic images.[49,50] Spectra showed clear Cu Kα lines confirming the presence of hot electrons. The penetration depth in CH was estimated to be 27 μm by comparing results from targets with plastic layers of different thickness. Using the online database ESTAR of NIST,[51] such penetration corresponds to an average hot electron energy ≈50 keV, in agreement with predictions from scaling laws[52] and available data.[53]

By measuring the total flux of Kα photons (with the CCD and the Kα imager), we could estimate the total number of hot electrons, finding a conversion efficiency from laser to hot electrons of less than 1%. This value is in agreement with what estimated in an experiment[54] carried out at the same laser facility.

As for the analysis of the backscattered light, a full account will be given elsewhere, and preliminary results are presented in Ref. 55. Here, we anticipate that back-reflection within the focusing lens cone was only a few % with the RPP. Without the RPP, it increased typically by a factor ≈2, for the same nominal intensity. The higher level of back-reflection without RPP might be due to non-uniformities in the spot enhancing the non-linear coupling, possibly driven by filamentation. Backscattering signal was dominated by emission close to the laser wavelength, although the spectral resolution was not sufficient to distinguish between SBS and purely reflected laser light. The scattered light outside the lens cone was estimated to be of the same order of that within the cone, using mini calorimeters placed in the interaction chamber. This leads to an estimated total reflectivity ≤15%. Clearly, such a measurement based on a few points is critical and needs to be refined in future experiments. SRS and TPD spectra were detected in the back-reflected light. SRS spectra are characterized by a Landau cut-off at short wavelengths ($\lambda \approx 670$ nm) and at long wavelengths extend to $\lambda \approx 750$ nm. No sign of SRS originating at $\approx n_c/4$ was found. This is probably the signature of strong delocalized absorption in the extended plasma corona. Alternatively, it could be explained invoking cavitation in the plasma, as discussed in Ref. 56. On the other hand, TPD was also detected implying that some laser light was reaching the $n_c/4$ layer.

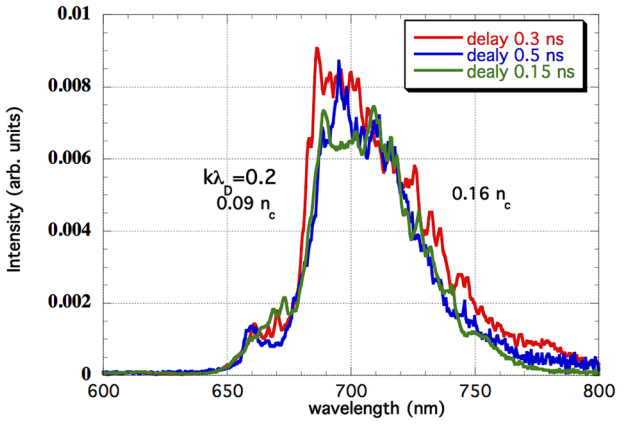

FIG. 4. Backreflected Raman spectra at three delays. The values 0.09 and 0.16 n_c correspond to the FWHM of the spectra.

In addition, as shown in Fig. 4, SRS spectra are only weakly dependent on delay, at least up to 600 ps. Shock breakout was also basically insensitive to the delay. Although a little surprising, this is probably due to the fact that the preformed plasma is too tenuous and cold to strongly affect energy deposition in the overdense plasma region.

V. DISCUSSION

Fig. 5 shows the shock breakout time vs. laser intensity for multilayered targets (a similar behavior was obtained for pure Cu targets). As expected, data obtained without phase plates show a larger scattering. However, the general trend is similar for such data too. Simulations results are also shown. The fit corresponds to scaling $\approx I^{-1/3}$ obtained by considering that, for stationary shocks in the classical regime, shock pressure $P \approx I^{2/3}$ and shock velocity $\approx P^{1/2}$.

As anticipated above, by matching experimental and simulated breakout times, we have shown that during the interaction we generate a shock pressure $P \approx 90$ Megabars. This is indeed the highest pressure obtained so far in this kind of experiment.[16,17,24,57] However, much higher

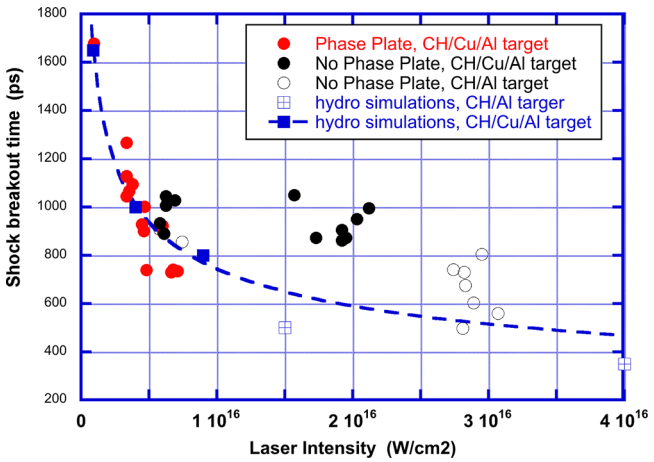

FIG. 5. Shock breakout times vs. laser intensity for different interaction and target conditions. Hydro simulation results are also shown (the actual intensity of simulation is half of what reported on the x-axis).

pressures were expected on the basis of known scaling-laws (1D models) and from simulations with nominal parameters. In order to reconcile experimental data and simulations, we considered several possibilities:

(1) Parametric instabilities bring to a large reflection and scattering of light, substantially reducing the energy available on target. However, we do measure a very small energy loss due to parametric instabilities within the cone lens (which is indeed quite large: $f/2$) and preliminary data indicate that the same happens outside this cone.
(2) Hot electrons alter the process of energy transport and shock generation. However, this does not seem compatible with the low conversion efficiency into hot electrons estimated in our experiment.
(3) The extended plasma corona brings to strong delocalized absorption limiting energy deposition in the denser plasma region. Indeed, this is certainly taking place (and probably confirmed by SRS spectra). However, there was no clear dependence of breakout time on delay (i.e., on corona extension) and even without the preformed plasma (main beam alone) this was the same, suggesting that the effect is not large in our experiment.
(4) Filamentation takes place in the corona and alters the conditions of interactions bringing to a larger spot diameter and reduced target intensity on target (filamentation threshold is surely exceed in our experimental conditions). However, the observed plasma size was compatible with the expected size of the focal spot. Also the hypothesis of strong filamentation does not seem to be compatible with the low observed scattering of laser light.
(5) In the intensity range explored in this experiment, the mechanisms of energy transport and shock formation differ from those in the "classical regime" (i.e., between 10^{13} and 10^{15} W/cm^2) bringing to different scaling laws, as predicted in recent theoretical works 58 and 59. Far from being exhaustive, such models show that a departure from the ablative scaling may be significant at high intensities.

In order to discriminate among all such possibilities, we performed an extended set of 2D hydrodynamics simulations retrieving shock breakout times obtained at different laser intensities. These reproduced the trend of experimental data vs. intensity (Fig. 5, which also shows the "classical" scaling of shock pressure, i.e., assuming a stationary shock, $t \approx I^{-1/3}$). Simulations also showed two additional very important aspects:

(1) The initial value of shock pressure during laser interaction is strongly affected by the spot size. The distance between the layers where laser light is absorbed and the ablation region ($\approx 60\,\mu$m) is comparable to spot size. Pressure is therefore decreased due to the lateral energy flow in the overcritical region. In order to evaluate such an effect, we performed simulations with exactly the same parameters but increased focal spot size, approaching a 1D ideal case. This considerably reduced the lateral flow and increased the pressure generated. For instance for the case previously cited (Fig. 3), we got a maximum pressure of $\approx$180 Megabars instead of 90 Megabars in the plastic layer, i.e., a factor $\approx$2. The effect and the pressure increase were similar for all investigated laser intensities.
[In order to evaluate this effect, one would really like to have a larger focal spot with the same intensity. But this would require an increased energy and here we meet a limitation due to the laser facility. Therefore, we performed hydro simulations where we fixed the laser intensity on target and then changed the focal spot size to see how the pressure changes. For small spots, the pressure is reduced, then by increasing the spot the pressure increases until it stabilize to that given by 1D model (or by 1D hydro simulations). The transition takes place typically when the focal spot diameter becomes comparable to the thickness of the overcritical region in the plasma (distance between the absorption region and the ablation front). When the radius reaches the value of the overcritical thickness, the shock pressure stop increasing and saturates. Indeed, this is exactly the condition at which one would expect that a 1D model become approximately applicable and valid].
(2) In order to reproduce experimental results (see Fig. 4), we needed to substantially cut the laser energy on target. The reduction was $\approx$50% of the "nominal" intensity, or a bit lower if all parameters are "stretched" to the extreme values allowed by experimental uncertainties (i.e., focal spot, pulse duration, and laser energy are all changed by 10%). Also simulations showed that only about 50% of incident laser light was absorbed in the plasma. This leaves us with the question of where $\approx$70% of laser light is disappearing. Possibly, light is refracted at very large angles in the corona and therefore it is not detected by our diagnostics neither inside the lens cone nor outside it. Clearly, as anticipated before, more measurements, including full angle absorption measurements, are needed to answer this question.

VI. CONCLUSIONS

Our experiment has shown that we can couple a laser beam to a payload and generate a rather strong shock (90 Megabars) even in the presence of an extended plasma corona. This is, indeed, the highest pressure measured so far in this kind of experiments, showing a clear progress in approaching a shock ignition relevant regime. Higher pressures (up to 180 Megabars) are inferred when a much larger focal spot is used.

Unlike experiments performed in spherical geometry,[17,18] we measured little back-reflection due to parametric instabilities and little generation of hot electrons. The results from other experiments,[24] also performed in planar geometry, although at lower intensity, are consistent with ours. This is indeed another matter, which must still be understood in order to progress towards an accurate modeling of shock ignition experiments.

Although our results showing high pressure and low parametric instabilities are good news for SI, one should be

cautious, since both growth rate and saturation of parametric instabilities critically depend on plasma conditions which, in our experiment, are quite different from a real SI experiment, especially concerning plasma scale-length and plasma temperature.

It is worth to discuss the effect of laser wavelength, i.e., what physics could be different when changing the laser wavelength from 438 nm to 351 nm, the wavelength at which ignition experiments are being attempted.

Indeed, for pellet compression, it is well-known that one must use short wavelengths in order to reduce target preheating (due to both electrons and X-rays) and increase hydrodynamic efficiency (i.e., maximize mass ablation rate and shock pressure generation). Now in shock ignition, target preheating is not such a sever issues because hot electrons are generated at the end of the compression. This indeed may re-open the way to the use of longer wavelength lasers, maybe even lasers working at 1ω (at least for the final laser spike). As for Laser Plasma Parametric Instabilities, or hot electron generation, we do not indeed expect many changes when moving from 438 to 351 nm. For instance, the threshold ($I\lambda^2$) increases from 351 nm to about 60%, but the physical processes are not so different. However, clearly more experiments are needed here.

ACKNOWLEDGMENTS

We acknowledge the support of HiPER project and Preparatory Phase Funding Agencies (EC, MSMT, and STFC). The work was also supported by the European Union under the "Laserlab" program of the 7th FP, by the Czech Ministry of Education, Youth and Sports, Project Nos. LC528 and LM2010014, by the Italian MIUR (Grants No. PRIN 2009FCC9MS and No. PRIN 2012AY5LEL), Sapienza University (Grant 2012 C26A12CZH2), and by the National Centre for Science (NCN), Poland, under Grant No. 2012/04/M/ST2/00452. SciTech Precision and Rutherford Appleton Laboratory Target Fabrication Group supplied targets. Finally, we thank the technical staff of PALS for help in running the experiments.

[1]R. Betti, C. D. Zhou, K. S. Anderson, L. J. Perkins, W. Theobald, and A. A. Solodov, Phys. Rev. Lett. **98**, 155001 (2007).
[2]L. J. Perkins, R. Betti, K. N. LaFortune, and W. H. Williams, Phys. Rev. Lett. **103**, 045004 (2009).
[3]X. Ribeyre, G. Schurtz, M. Lafon, S. Galera, and S. Weber, Plasma Phys. Controlled Fusion **51**, 015013 (2009).
[4]S. Atzeni, A. Schiavi, and A. Marocchino, Plasma Phys. Controlled. Fusion **53**, 035010 (2011).
[5]S. Atzeni and G. Schurtz, Proc. SPIE **8080**, 808022 (2011).
[6]J. Nuckolls, L. Wood, A. Thiessen, and G. Zimmerman, Nature **239**, 139 (1972).
[7]J. Lindl, Phys. Plasmas **2**, 3933 (1995).
[8]S. Atzeni and J. Meyer-ter-Vehn, *The Physics of Inertial Fusion* (Clarendon-Oxford, 2004).
[9]H. Azechi, T. Jitsuno, T. Kanabe, M. Katayama, K. Mima, N. Miyanaga, M. Nakai, S. Nakai, H. Nakaishi, M. Nakatsuka, A. Nishiguchi, P. A. Norrays, Y. Setsuhara, M. Takagi, M. Yamanaka, and C. Yamanaka, Laser Part. Beams **9**, 193 (1991).
[10]T. C. Sangster, V. N. Goncharov, R. Betti, T. R. Boehly, D. T. Casey, T. J. B. Collins, R. S. Craxton, J. A. Delettrez, D. H. Edgell, R. Epstein, K. A. Fletcher, J. A. Frenje, Y. Yu. Glebov, D. R. Harding, S. X. Hu, I. V. Igumenschev, J. P. Knauer, S. J. Loucks, C. K. Li, J. A. Marozas, F. J. Marshall, R. L. McCrory, P. W. McKenty, D. D. Meyerhofer, P. M. Nilson, S. P. Padalino, R. D. Petrasso, P. B. Radha, S. P. Regan, F. H. Seguin, W. Seka, R. W. Short, D. Shvarts, S. Skupsky, V. A. Smalyuk, J. M. Soures, C. Stoeckl, W. Theobald, and B. Yaakobi, Phys. Plasmas **17**, 056312 (2010).
[11]O. L. Landen, R. Benedetti, D. Bleuel, T. R. Boehly, D. K. Bradley, J. A. Caggiano, D. A. Callahan, P. M. Celliers, C. J. Cerjan, D. Clark, G. W. Collins, E. L. Dewald, S. N. Dixit, T. Doeppner, D. Edgell, J. Eggert, D. Farley, J. A. Frenje, V. Glebov, S. M. Glenn, S. H. Glenzer, S. W. Haan, A. Hamza, B. A. Hammel, C. A. Haynam, J. H. Hammer, R. F. Heeter, H. W. Herrmann, D. G. Hicks, D. E. Hinkel, N. Izumi, M. Gatu Johnson, O. S. Jones, D. H. Kalantar, R. L. Kauffman, J. D. Kilkenny, J. L. Kline, J. P. Knauer, J. A. Koch, G. A. Kyrala, K. LaFortune, T. Ma, A. J. Mackinnon, A. J. Macphee, E. Mapoles, J. L. Milovich, J. D. Moody, N. B. Meezan, P. Michel, A. S. Moore, D. H. Munro, A. Nikroo, R. E. Olson, K. Opachich, A. Pak, T. Parham, P. Patel, H.-S. Park, R. P. Petrasso, J. Ralph, S. P. Regan, B. A. Remington, H. G. Rinderknecht, H. F. Robey, M. D. Rosen, J. S. Ross, J. D. Salmonson, T. C. Sangster, M. B. Schneider, V. Smalyuk, B. K. Spears, P. T. Springer, L. J. Suter, C. A. Thomas, R. P. J. Town, S. V. Weber, P. J. Wegner, D. C. Wilson, K. Widmann, C. Yeamans, A. Zylstra, M. J. Edwards, J. D. Lindl, L. J. Atherton, W. W. Hsing, B. J. MacGowan, B. M. Van Wonterghem, and E. I. Moses, Plasma Phys. Controlled Fusion **54**, 124026 (2012).
[12]S. W. Haan, J. D. Lindl, D. A. Callahan, D. S. Clark, J. D. Salmonson, B. A. Hammel, L. J. Atherton, R. C. Cook, M. J. Edwards, S. Glenzer, A. V. Hamza, S. P. Hatchett, M. C. Herrmann, D. E. Hinkel, D. D. Ho, H. Huang, O. S. Jones, J. Kline, G. Kyrala, O. L. Landen, B. J. MacGowan, M. M. Marinak, D. D. Meyerhofer, J. L. Milovich, K. A. Moreno, E. I. Moses, D. H. Munro, A. Nikroo, R. E. Olson, K. Peterson, S. M. Pollaine, J. E. Ralph, H. F. Robey, B. K. Spears, P. T. Springer, L. J. Suter, C. A. Thomas, R. P. Town, R. Vesey, S. V. Weber, H. L. Wilkens, and D. C. Wilson, Phys. Plasmas **18**, 051001 (2011).
[13]E. Moses and C. R. Craig, Fusion Sci. Technol. **47**(3), 314 (2005).
[14]M. Tabak, D. S. Clark, S. P. Hatchett, M. H. Key, B. F. Lasinski, R. A. Snavely, S. C. Wilks, R. P. J. Town, R. Stephens, E. M. Campbell, R. Kodama, K. Mima, K. A. Tanaka, S. Atzeni, and R. Freeman, Phys. Plasmas **12**, 057305 (2005).
[15]W. Theobald, A. A. Solodov, C. Stoeckl, K. S. Anderson, R. Betti, T. R. Boehly, R. S. Craxton, J. A. Delettrez, C. Dorrer, J. A. Frenje, V. Yu. Glebov, H. Habara, K. A. Tanaka, J. P. Knauer, R. Lauck, F. J. Marshall, K. L. Marshall, D. D. Meyerhofer, P. M. Nilson, P. K. Patel, H. Chen, T. C. Sangster, W. Seka, N. Sinenian, T. Ma, F. N. Beg, E. Giraldez, and R. B. Stephens, Phys. Plasmas **18**, 056305 (2011).
[16]K. S. Anderson, R. Betti, P. W. McKenty, T. J. B. Collins, M. Hohenberger, W. Theobald, R. S. Craxton, J. A. Delettrez, M. Lafon, J. A. Marozas, R. Nora, S. Skupsky, and A. Shvydky, Phys. Plasmas **20**, 056312 (2013).
[17]W. Theobald, R. Betti, C. Stoeckl, K. S. Anderson, J. A. Delettrez, V. Yu. Glebov, V. N. Goncharov, F. J. Marshall, D. N. Maywar, R. L. McCrory, D. D. Meyerhofer, P. B. Radha, T. C. Sangster, W. Seka, D. Shvarts, V. A. Smalyuk, A. A. Solodov, B. Yaakobi, C. D. Zhou, J. A. Frenje, C. K. Li, F. H. Séguin, R. D. Petrasso, and L. J. Perkins, Phys. Plasmas **15**, 056306 (2008).
[18]W. Theobald, K. S. Anderson, R. Betti, R. S. Craxton, J. A. Delettrez, J. A. Frenje, V. Yu Glebov, O. V. Gotchev, J. H. Kelly, C. K. Li, A. J. Mackinnon, F. J. Marshall, R. L. McCrory, D. D. Meyerhofer, J. F. Myatt, P. A. Norrays, P. M. Nilson, P. K. Patel, R. D. Petrasso, P. B. Radha, C. Ren, T. C. Sangster, W. Seka, V. A. Smalyuk, A. A. Solodov, R. B. Stephens, C. Stoeckl, and B. Yaakobi, Plasma Phys. Controlled Fusion **51**, 124052 (2009).
[19]P. B. Radha, R. Betti, T. R. Boehly, J. A. Delettrez, D. H. Edgell, V. N. Goncharov, I. V. Igumenshchev, J. P. Knauer, J. A. Marozas, F. J. Marshall, R. L. McCrory, D. D. Meyerhofer, S. P. Regan, T. C. Sangster, W. Seka, S. Skupsky, A. A. Solodov, C. Stoeckl, W. Theobald, J. A. Frenje, D. T. Casey, C. K. Li, and R. D. Petrasso, IEEE Trans. Plasma Sci. **39**, 1007 (2011).
[20]D. Besnard, Eur. Phys. J. D **44**, 207–213 (2007).
[21]W. Seka, E. A. Williams, R. S. Craxton, L. M. Goldman, R. W. Short, and K. Tanaka, Phys. Fluids **27**, 2181 (1984).
[22]T. Afshar-rad, L. A. Gizzi, M. Desselberger, F. Khattak, O. Willi, and A. Giulietti, Phys Rev. Lett. **68**, 942 (1992).
[23]K. Tanaka, L. M. Goldman, W. Seka, M. C. Richardson, J. M. Soures, and E. A. Williams, Phys. Rev. Lett. **48**, 1179 (1982).

[24]A. Giulietti, A. Macchi, E. Schifano, V. Biancalana, C. Danson, D. Giulietti, L. A. Gizzi, and O. Willi, Phys. Rev E **59**(1), 1038 (1999).
[25]S. Yu. Gus'kov, N. N. Demchenko, A. Kasperczuk, T. Pisarczyk, Z. Kalinowska, T. Chodukowski, O. Renner, M. Smid, E. Krousky, M. Pfeifer, J. Skala, J. Ullschmied, and P. Pisarczyk, "Laser-driven ablation through fast electrons in PALS-experiment at the laser radiation intensity of 1–50 PW/cm^2," Laser Part. Beams **32**, 177 (2014).
[26]S. D. Baton, M. Koenig, E. Brambrink, H. P. Schlenvoigt, C. Rousseaux, G. Debras, S. Laffite, P. Loiseau, F. Philippe, X. Ribeyre, and G. Schurtz, Phys. Rev. Lett. **108**, 195002 (2012).
[27]K. Jungwirth, A. Cejnarova, L. Juha, B. Kralikova, J. Krasa, E. Krousky, P. Krupickova, L. Laska, K. Masek, T. Mocek, M. Pfeifer, A. Präg, O. Renner, K. Rohlena, B. Rus, J. Skala, P. Straka, and J. Ullschmied, Phys. Plasmas **8**, 2495 (2001).
[28]L. Antonelli, D. Batani, A. Patria, O. Ciricosta, C. Cecchetti, P. Koester, L. Labate, A. Giulietti, L. A. Gizzi, A. Moretti, M. Richetta, L. Giuffrida, L. Torrisi, M. Kozlova, J. Nejdl, M. Sawicka, D. Margarone, B. Rus, G. Schurtz, X. Ribeyre, M. Lafon, C. Spindloe, and T. O'Dell, Acta Tech. **56**, T57 (2011).
[29]D. Batani, G. Malka, G. Schurtz, X. Ribeyre, E. Lebel, L. Giuffrida, V. Tikhonchuk, L. Volpe, A. Patria, P. Koester, L. Labate, L. A. Gizzi, L. Antonelli, M. Richetta, J. Nejdl, M. Sawicka, D. Margarone, M. Krus, E. Krousky, J. Skala, R. Dudzak, A. Velyhan, J. Ullshmied, O. Renner, M. Smid, O. Klimo, S. Atzeni, A. Marocchino, A. Schiavi, C. Spindloe, T. O'Dell, T. Vinci, J. Wolowski, J. Badziak, T. Pisarczyk, M. Rosinski, Z. Kalinowska, and T. Chodukowski, J. Phys.: Conf. Ser. **399**, 012005 (2012).
[30]B. Rus, T. Mocek, A. R. Präg, M. Kozlová, G. Jamelot, A. Carillon, D. Ros, D. Joyeux, and D. Phalippou, Phys. Rev. A **66**, 063806 (2002).
[31]M. Koenig, B. Faral, J. M. Boudenne, D. Batani, S. Bossi, A. Benuzzi, C. Remond, J. Perrine, M. Temporal, and S. Atzeni, Phys. Rev. Lett. **74**, 2260 (1995).
[32]D. Batani, H. Stabile, A. Ravasio, G. Lucchini, T. Desai, J. Ullschmied, E. Krousky, L. Juha, J. Skala, B. Kralikova, M. Pfeifer, C. Kadlec, T. Mocek, A. Präg, H. Nishimura, and Y. Ochi, Phys. Rev. E **68**, 067403 (2003).
[33]A. Morace and D. Batani, Nucl. Instrum. Method A **623**, 797 (2010).
[34]T. Pisarczyk, S. Yu. Gus'kov, Z. Kalinowska, J. Badziak, D. Batani, L. Antonelli, G. Folpini, Y. Maheut, F. Baffigi, S. Borodziuk, T. Chodukowski, G. Cristoforetti, N. N. Demchenk, L. A. Gizz, A. Kasperczuk, P. Koester, E. Krousky, L. Labat, P. Pary, M. Pfeifer, O. Renner, M. Smid, M. Rosinski, J. Skala, R. Dudzak, J. Ullschmied, and P. Pisarczyk, Phys. Plasmas **21**, 012708 (2014).
[35]M. Šmíd, L. Antonelli, and O. Renner, Acta Polytech. **53**, 233 (2013).
[36]J. Nejdl and M. Kozlová, Proc. SPIE **7451**, 745117 (2009).
[37]R. Ramis, R. Schmalz, and J. Meyer-ter Vehn, Comput. Phys. Commun. **49**, 475 (1988).
[38]R. Ramis, J. Meyer-ter-Vehn, and J. Ramírez, Comput. Phys. Commun. **180**, 977 (2009).
[39]S. Atzeni, Comput. Phys. Commun. **43**, 107 (1986).
[40]S. Atzeni, A. Marocchino, A. Schiavi, and G. Schurtz, Comput. Phys. Commun. **169**, 153 (2005).
[41]P. H. Maire, R. Abgrall, J. Breil, and J. Ovadia, SIMA J. Sci. Comput. **29**, 1781 (2007).
[42]H. K. Chung, M. H. Chen, W. L. Morgan, Y. Ralchenko, and R. W. Lee, High Energy Density Phys. **1**, 3 (2005).
[43]J. J. MacFarlane, I. E. Golovkin, P. Wang, P. R. Woodruff, and N. A. Pereyra, High Energy Density Phys. **3**, 181 (2007).
[44]A. Picciotto, J. Krása, L. Láska, K. Rohlena, L. Torrisi, S. Gammino, A. M. Mezzasalma, and F. Caridi, Nucl. Instrum. Methods B **247**, 261 (2006).
[45]D. Margarone, J. Krása, L. Giuffrida, A. Picciotto, L. Torrisi, T. Nowak, P. Musumeci, A. Velyhan, J. Prokůpek, L. Láska, T. Mocek, J. Ullschmied, and B. Rus, J. Appl. Phys. **109**, 103302 (2011).
[46]SESAME Report on the Los Alamos Equation of State Library, Report No. LALP-83-4, 1983.
[47]T. Levato, L. Labate, N. Pathak, C. A. Cecchetti, P. Koester, E. Di Fabrizio, P. Delogu, A. Giulietti, D. Giulietti, and L. A. Gizzi, Nucl. Instrum. Methods A **623**, 842 (2010).
[48]L. Gizzi, A. Giulietti, D. Giulietti, P. Köster, L. Labate, T. Levato, F. Zamponi, A. Lübcke, T. Kämpfer, I. Uschmann, E. Förster, A. Antonicci, and D. Batani, Plasma Phys. Controlled Fusion **49**, B211 (2007).
[49]L. Labate, P. Koester, T. Levato, and L. A. Gizzi, Rev. Sci. Instrum. **83**, 103504 (2012).
[50]F. Zamponi, F. Zamponi, A. Lübcke, T. Kämpfer, I. Uschmann, E. Förster, A. P. L. Robinson, A. Giulietti, P. Köster, L. Labate, T. Levato, and L. A. Gizzi, Phys. Rev. Lett. **105**, 085001 (2010).
[51]See http://physics.nist.gov/PhysRefData/Star/Text/ESTAR.html for Estar database.
[52]F. N. Beg, A. R. Bell, A. E. Dangor, C. N. Danson, A. P. Fews, M. E. Glinsky, B. A. Hammel, P. Lee, P. A. Norreys, and M. Tatarakis, Phys. Plasmas **4**, 447 (1997).
[53]C. Rousseaux, F. Amiranoff, C. Labaune, and G. Matthieussent, Phys. Fluids B **4**, 2589 (1992).
[54]S. Guskov, S. Borodziuk, M. Kalal, A. Kasperczuk, V. N. Kondrashov, J. Limpouch, P. Pisarczyk, T. Pisarczyk, K. Rohlena, J. Skala, and J. Ullschmied, J. Russ. Laser Res. **26**(3), 228 (2005).
[55]P. Koester, L. Antonelli, S. Atzeni, J. Badziak, F. Baffigi, D. Batani, C. A. Cecchetti, T. Chodukowski, F. Consoli, G. Cristoforetti, R. De Angelis, G. Folpini, L. A. Gizzi, Z. Kalinowska, E. Krousky, M. Kucharik, L. Labate, T. Levato, R. Liska, G. Malka, Y. Maheut, A. Marocchino, T. O'Dell, P. Parys, T. Pisarczyk, P. Raczka, O. Renner, Y. J. Rhee, X. Ribeyre, M. Richetta, M. Rosinski, L. Ryc, J. Skala, A. Schiavi, G. Schurtz, M. Smid, C. Spindloe, J. Ullschmied, J. Wolowski, and A. Zaras, Plasma Phys. Controlled Fusion **55**, 124045 (2013).
[56]O. Klimo, S. Weber, V. T. Tikhonchuk, and J. Limpouch, Plasma Phys. Controlled Fusion **52**, 055013 (2010).
[57]D. Batani, S. Baton, A. Casner, S. Depierreux, M. Hohenberger, O. Klimo, M. Koenig, C. Labaune, X. Ribeyre, C. Rousseaux, G. Schurtz, W. Theobald, and V. T. Tikhonchuk, "Physical issues in shock ignition," Nucl. Fusion (2012) (to be published).
[58]A. R. Bell and M. Tzoufras, Plasma Phys. Controlled Fusion **53**, 045010 (2011).
[59]S. Guskov, X. Ribeyre, M. Touati, J.-L. Feugeas, Ph. Nicolaï, and V. Tikhonchuk, Phys. Rev. Lett. **109**, 255004 (2012).